

Discovery of Iron Group Impurity Ion Spin States in Single Crystal Y_2SiO_5 with Strong Coupling to Whispering Gallery Photons

Maxim Goryachev,¹ Warrick G. Farr,¹ Natalia C. Carvalho,¹ Daniel L. Creedon,¹ Jean-Michel Le Floch,¹ Sebastian Probst,² Pavel Bushev,³ and Michael E. Tobar^{1,*}

¹*ARC Centre of Excellence for Engineered Quantum Systems,
School of Physics, University of Western Australia,
35 Stirling Highway, Crawley WA 6009, Australia*

²*Physikalisches Institut, Karlsruhe Institute of Technology, D-76128 Karlsruhe, Germany*

³*Experimentalphysik, Universität des Saarlandes, D-66123 Saarbrücken, Germany*

(Dated: June 13, 2022)

Interaction of Whispering Gallery Modes (WGM) with dilute spin ensembles in solids is an interesting paradigm of Hybrid Quantum Systems potentially beneficial for Quantum Signal Processing applications. New transitions are measured in single crystal Y_2SiO_5 using WGM spectroscopy with large Zero Field Splittings at 14.7GHz, 18.4GHz and 25.4GHz, which also feature considerable anisotropy of the g-tensors, as well as two inequivalent lattice sites, indicating spins from Iron Group Ion (IGI) impurities. The comparison of undoped and Rare-Earth doped crystals reveal that the IGIs are introduced during co-doping of Eu or Er with concentration at much lower levels of order 100 ppb. The strong coupling regime between an ensemble of IGI spins and WGM photons have been demonstrated at 18.4 GHz and near zero field. This approach together with useful optical properties of these ions opens a new avenue for 'spins-in-solids' Quantum Electrodynamics.

The development of Hybrid Quantum Systems (HQS) has become a promising direction towards the realisation of the quantum information processing unit[1–4]. Such systems gather together the advantages of its constituting parts, which are based on different physical systems in the quantum regime. Examples include superconducting qubits, trapped atoms, electron and atomic spins, etc. These systems usually require either an optical or microwave electromagnetic coherent readout, usually based on photonic cavities both 2D and 3D. Despite recent progress in 2D planar superconducting structures, some advantages of 3D superconducting cavities, such as long coherence time of specially design transmons[5, 6] and very high Q -factors, revive recent attention to these structures [7]. Some examples of 3D cavities include; Transverse Electric (TE) [7, 8], lumped reentrant[9, 10], Fabry-Pérot (FP)[11, 12] and Whispering Gallery Mode (WGM)[13–17] resonators. Up to now, HQS were based only on TE, lumped and FP type resonators[7]. In this work we demonstrate that the strong coupling regime required for coherent quantum information readout can also be achieved using microwave WGM photons interacting with spins in a dielectric.

WGMs are widely used as a probing tool in many areas of science including detection of mechanical motion[18], magnetic fields[19], biological substances[20], test of fundamental physics[21], and are now approaching quantum limited sensitivity[22]. Whispering Gallery modes are also used as classical[23, 24] and atomic[25, 26] oscillators. The popularity of these types of resonators is due to the possibility of achieving extremely high Quality Factors through the elimination of most loss terms excluding the material loss[27]. Recently, these types of modes have been used for ultrasensitive microwave spectroscopy of

paramagnetic impurities in dielectric crystals[14–17] with efficient sensitivity to detect naturally occurring impurities at the level of few parts per billion.

In a typical WGM resonator, electromagnetic energy is mostly confined within the dielectric crystal simultaneously hosting impurity ions and playing a role of a 3D photonic cavity. This solution is potentially advantageous over a 2D cavity where the host crystal is placed in the evanescent field of a metallic structure, since it may result in stronger coupling with lower cavity loss. For example, WGMs in low loss crystals, such as sapphire (Al_2O_3), allows the cavity Quality Factors of more than a billion, whereas the superconducting 2D and 3D resonators nowadays are limited by a few million[6, 28, 29].

The strong coupling regime in microwave WGM cavities has yet to be demonstrated clearly due to the large linewidths of the Electron Spin Resonance (ESR) studied to date, in particular sapphire has extremely low loss, allowing WGMs to have Q -factors at the single photon level of one hundred million (10 Hz linewidth)[30]. However the nuclei spins of the Al^{3+} lattice ions broaden the ESR for Fe^{3+} to around 28 MHz[31]. Improvement in the ESR width can be made by changing the crystal host and type of an ion constituting the spin ensemble at the expense of the photon Q -factor.

Single crystal Y_2SiO_5 (YSO) is a potential candidate for this role due for a number of reasons. Firstly, YSO is a low loss biaxial dielectric with a large enough dielectric constant (of order 10)[32]. Such features of this crystal make it possible to design low loss 3D WGM type cavities in the X and K_u frequency bands. Secondly, Er^{3+} ions in YSO crystal both have microwave (magnetic field controllable over the X and K_u bands) and infrared optical (telecommunication C-band) transitions exhibit-

ing long coherence times[33]. Thirdly, ^{167}Er isotope has nonzero nuclear spin resulting in a hyperfine structure occupying 1-5 GHz range at zero external field[34]. Due to combination of these microwave and optical properties, doped YSO crystals have recently drawn considerable attention in quantum optical community[35–37]. Potentially, they can be used for the physical realisation of microwave quantum memories[38, 39] and microwave-optical quantum interface[1, 40–43].

WGM resonators have been considered as microwave-to-optical up converters with one photon efficiency[44]. Despite the dominant role of Rare Earth dopings of YSO crystals for optical applications, the Iron Group Ions (IGIs) could also play an important role in some optical devices[45]. In this work we discover a significant amount of unintentionally introduced spin impurities in Erbium and Europium doped single crystal ($\text{Er}^{3+}:\text{Y}_2\text{SiO}_5$, $\text{Eu}^{3+}:\text{Y}_2\text{SiO}_5$) which we attribute to IGIs due to existence of large Zero Field Splittings (ZFS). We also observe some degree of magnetic anisotropy of these ions and demonstrate the strong coupling regime for an ensemble of IGIs. These ion impurities are unintentional co-dopants with the Rare-Earth Ions (REIs) introduced during the crystal growth process.

We believe that, IGIs can be very useful in the field of hybrid quantum systems. Many of Iron Group Ions implemented in solids have both optical (mostly visible) and microwave transitions that makes them interesting for quantum limited frequency conversion. Moreover, the IGIs possess often a ZFS in microwave working range of aluminium superconducting (SC) qubits. Thus, as in the case with nitrogen vacancy in diamond[46], only weak magnetic field is required to tune the spins in resonance with qubits. Thus, achieving the strong coupling regimes between dilute IGIs in solids with photons is an interesting new area of investigation.

Several cylindrically shaped YSO crystals (see Table I for details) were placed in a copper shield situated in a superconducting magnet (see Fig. 1), with all samples grown by Scientific Materials Corp. The system was cooled down to 20 mK with a dilution refrigerator. The WGMs in the dielectric cavity were coupled to the electric components of the field with two straight probes. This coupling is kept low in order to prevent external losses. The incident signal is cryogenically attenuated by 10, 10 and 20 dB at 4K, 100mK and 20mK cryocooler stages respectively. This attenuation prevent penetration of the room temperature noise into the system. The output signal is amplified by a low noise cryogenic amplifier cooled to 4K and another room-temperature amplifier. The cavity and the cold amplifier are separated by a circulator at the 20mK stage preventing the amplifier back-action. For all the experiment the external DC magnetic field is applied along the symmetry axis of the resonator cylinder.

The experimental procedure presuppose scanning of

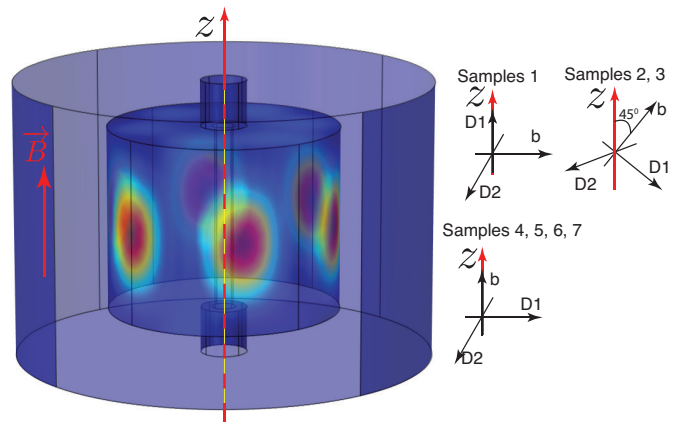


FIG. 1: Simulation of a WGM in a YSO crystal inside a metallic cavity in terms of energy density, crystal axes orientation with respect to cylinder axes.

the external DC magnetic field and monitoring the cavity response[14, 15]. When the splitting between energy levels approaches the WGM resonance frequency, the system exhibits an avoided crossing between two Harmonic Oscillators: one is the photon mode, the other is the spin ensemble[47]. If the coupling strength between a spin ensemble and a photonics mode exceeds the average linewidth of the resonances, the system is said to exhibit the strong coupling regime. This regime is characterised by hybridisation of the electromagnetic mode and the spin ensemble and is fruitful for many applications of quantum signal processing[48].

Fig. 2, (1A) and (1B), demonstrates the strong coupling regime between a Whispering Gallery Magnetic Mode ($\text{WGH}_{1,2,1}$) at $\frac{\omega_0}{2\pi} = 18.436$ GHz with Q -factor of 3.7×10^4 and the g_{2+} spins. The corresponding coupling between the spin ensemble and the WGM photons is $\frac{g}{\pi} \approx 3.3$ MHz which is greater than mean linewidth of the ensemble and WGMs $2\delta = \delta_{\text{WGM}} + \Gamma_2^* \approx 1.9$ MHz where standalone Γ_2^* is 1.4 MHz. The corresponding average concentration of spins in the lower energy state can be estimated as follows:

$$n = \frac{4\hbar}{\omega_0 \mu_0 \xi} \left(\frac{g}{g_{DC} \beta} \right)^2, \quad (1)$$

where ξ is the filling factor, g_{DC} is the DC g -factor, β is the Bohr magnetron. The simulated filling factor for the $\text{WGH}_{1,2,1}$ is 0.5 giving the corresponding concentration of the ions $4.5 \times 10^{15} \text{ cm}^{-3}$ which is significantly less than the expected concentration of Er ions. It should be noted that the external DC magnetic field at which the strong coupling regime is achieved is 2.5mT. This value is lower than the critical field for the superconducting phase of Aluminium, and very favorable for the direct integration with aluminium SC quantum circuits[46, 49]. Observed photon Q -factors for both doped and undoped crystals is on the order of 10^5 that is

less than that for the state-of-the-art 2D and 3D superconducting resonators[6, 28, 29], but could be potentially improved in larger crystals with better filling factors. Such moderate Q -factors make it impossible to observe degradation of the cavity linewidths due to the doping.

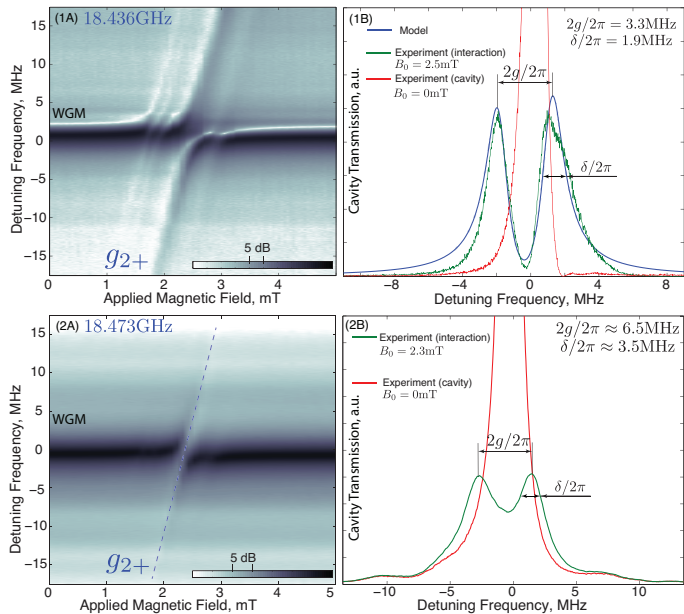


FIG. 2: Interaction between WGM photons and IGI spins for (1) Sample 4 ($f_0 = 18.436$ GHz) and (2) Sample 7 ($f_0 = 18.473$ GHz) demonstrated as a power transmission through the cavity as a function of frequency and external magnetic field (A) and as a function of detuning frequency at the interaction field (B). The strong coupling regime demonstrated at (1).

The result of the experimental procedure described above can be represented by a number of avoided level crossings (ALCs) such as those shown in Fig. 2. The ALCs can be put on a map where each dot denotes a crossing. Such a map is possible due to a large number of WGMs in a dielectric cylinder and their relatively narrow linewidths and high filling factors[14]. A map of ALCs attributed only to the IGIs for two Er:YSO (samples 4 and 2), and Eu:YSO (sample 7), are shown in Fig. 3 (A), (B) and (C) respectively, with corresponding Zeeman line interpretations. While the numerical parameter estimations for all seven samples are given in Table I. Classification of these ALCs as IGIs is apparent from the structure of the plotted transitions, which exhibit large Zero Field splittings due to the crystal field significantly affecting the 3d electrons. In contrast, REIs have shielded 4f electrons resulting in the absence of ZFS for isotopes with zero nuclear spin. These measurements have been compared to spectroscopy of a similar but undoped and purified crystal. This crystal demonstrates no ALCs from either REIs or IGIs. This suggests that both types of ions are introduced during the crystal growth

and doping process for both the Erbium or Europium doped crystals. Note that IGI co-doping has not been previously observed[7, 34, 50]. Thus, this work is the first demonstration of a strong coupling regime with the IGIs.

Not all ALCs can be classified as the strong coupling interaction due to mode differences in filling factors, polarisation and quality factors. Moreover, it is observed that typical coupling at larger external magnetic field is weaker than at lower ones due to the merging of spin ensembles in frequency space.

Spectroscopy in Fig 2 reveals the existence of three zero field splittings and five Kramers doublets. ZFS₁ appears at 25.4GHz and corresponds to ESR lines g_{1+} and g_{1-} , ZFS_{2,3} appear at 18.4GHz and corresponds to lines $g_{2\pm}$ and $g_{3\pm}$, ZFS_{4,5} is at 14.7GHz and corresponds to ESR lines $g_{4\pm}$ and $g_{5\pm}$. Figure 2a contains spectroscopic data taken when the magnetic field is parallel to the crystal axis. Therefore, all magnetically inequivalent positions merge. Since, no other ZFS has been found in the frequency range up to 30GHz and also we found no evidence of ALC between spin states (as has been observed for Fe³⁺ in sapphire[14]), we conclude that observed spectrum is due to the impurities with $S = 1$ and $S = \frac{3}{2}$.

We consider Cr, Ni and Fe ions as possible IGI impurities found in our spectroscopic measurements. There is evidence that the Chromium substitutes both the Y (octahedral site) and Si (tetrahedral site) with 3+ and 4+ valence states respectively. In particular, there are some ESR studies of such materials, especially Cr⁴⁺:YSO[51, 52], although detailed ESR spectroscopy of Cr:YSO is missing. Cr³⁺ has $S = \frac{3}{2}$ and Cr⁴⁺ has $S = 1$. Ni²⁺ possess $S = 1$ and does exist in 4-fold coordination and could theoretically (and at low levels) substitute for Si⁴⁺ ions accompanied by an Oxygen vacancy for charge balance. Fe⁶⁺ atomic radius is well matched to the Si⁴⁺ radius, and this ion exists in the 4-fold coordination, however its $S = \frac{1}{2}$. Fe⁴⁺ could also be excluded based on the fact[53, 54] that the corresponding atomic radius is much larger than the native Si⁴⁺, and it exists only in 6-fold coordination, rather than the native 4-fold of the Si site. Fe³⁺ is not reported to exist in the coordination of the two native Y³⁺ sites, 7-fold and 9-fold coordination. Fe²⁺ with $S = 3$ would yield complex ESR spectrum consisting of 3 Kramers doublets, one singlet state and many ALCs between spin states[14].

Summarising this information with regards to the observed ZFS (Table I), it can be concluded 1) ZFS₁ (25.4 GHz) belongs to $S = 1$ system which is most probably the Cr⁴⁺ ion; 2) ZFS₂, ZFS₃ (18.4 GHz) most likely belongs to Ni²⁺, $S = 1$ system; 3) ZFS₄, ZFS₅ (14.7 GHz) is expected to be Cr³⁺ giving $S = 3/2$ structure.

Despite the fact that the g -tensor is almost symmetric for IGIs, the observed ALCs demonstrate considerable dependence of on the crystal orientation. Indeed, in the

TABLE I: Details of the crystal samples, corresponding Zero Field Splittings (ZFS), g-factors and spin linewidths Γ_2^* . Crystal dimensions are given in by radius R and height h and serial number by S/N.

Sample	1	2	3	4	5	6	7
Orientation	D1 z	$\widehat{z}\widehat{b} = 45^\circ$	$\widehat{z}\widehat{b} = 45^\circ$	b z	b z	b z	b z
Doping, %	Er ³⁺ :0.005	Er ³⁺ :0.001	Er ³⁺ :0.005	Er ³⁺ :0.001	Er ³⁺ :0.001	Er ³⁺ :0.005	Eu ³⁺ :0.01
$R \times h$, mm	6×10	5×10	6×10	5×10	5×10	5×7.67	5×10
S/N	2-736-19	10-117-03	2-736-18	1-554-11	1-554-13	6-249-09	2-427-06
$\Gamma_2^*/2\pi$, MHz			1..2	1.4	1.1		2.2
ZFS ₁ , GHz				25.44			
$g_{1\pm}$				2.10/-2.22			
ZFS ₂ , GHz	18.38	18.38	18.36 ^a	18.38	18.38	18.43	18.38
$g_{2\pm}$	1.94/ND ^c	1.87/-2.25	1.86/-1.97	2.00/-2.29	2.00/-2.21	1.95/ND ^c	2.04/-2.32
ZFS ₃ , GHz		18.36	18.38 ^a				
$g_{3\pm}$		0.74/ND ^c	0.63/-1.03				
ZFS ₄ , GHz	14.69	14.70	14.71	14.68	14.74	14.74	14.69
$g_{4\pm}$	5.19/-4.38	5.21/-4.77	5.06/-4.55	4.05/-3.71	4.02/-4.00	3.78/-3.77	4.04/-3.71
ZFS ₅ , GHz	14.68	14.67	14.72	14.72	14.70	14.71	14.68
$g_{5\pm}$	2.24/-2.24 ^b	4.58/-3.72	4.41/ND ^c	1.75/-1.40	1.74/-1.42	1.76/-1.51	ND ^c /-1.4

^a Estimated with one interaction point.

^b Prominent quadratic dependence of the splitting on the magnetic field.

^c Not Detected.

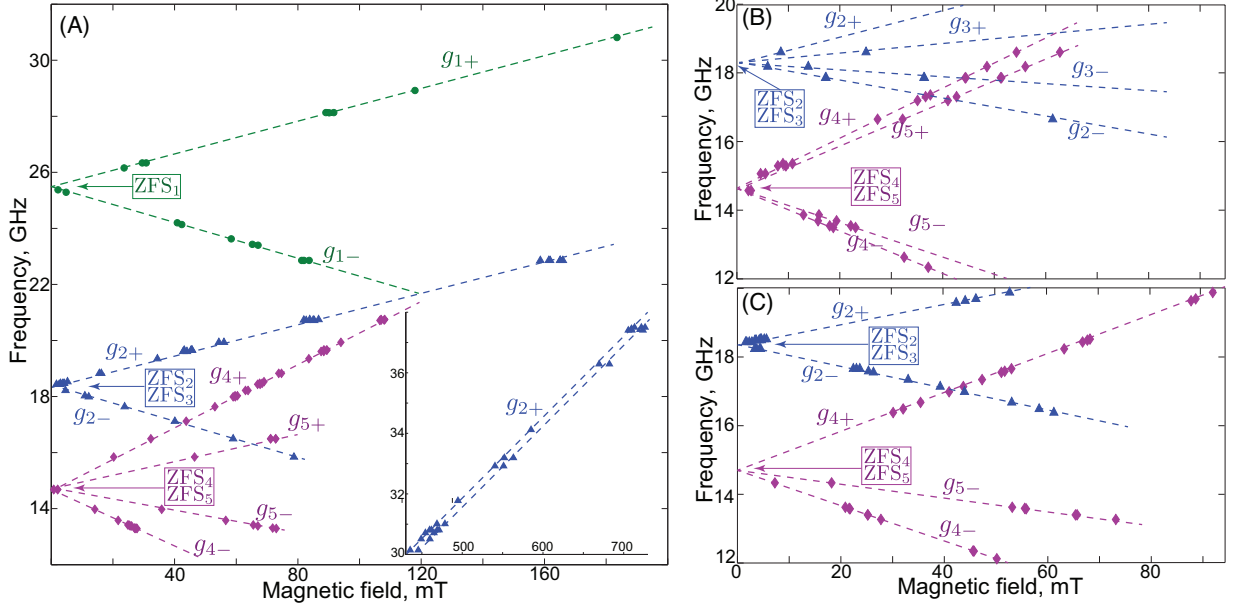


FIG. 3: Interactions of IGI magnetic impurities of YSO crystals with WGM at 20 mK with variation of the external DC magnetic field: (A) Sample 4 (The inset shows splitting of the g_{2+} line), (B) Sample 2, (C) Sample 7. Erbium and Europium transitions are not shown.

case of the $g_{5\pm}$ lines, the effective DC g-factor changes by around the factor of two when the crystal axes are rotated by 45° angle. Table I shows that this dependence is consistent for crystals with the same orientation and different doping level. Although almost symmetrical g-tensors are typical for IGIs, the literature provides a few examples of significant magnetic anisotropy of IGIs in solids[55].

Another feature that is not typical for IGIs is the splitting of the interactions into two lines at high field as

shown for g_{2+} on the inset of Fig. 3. This splitting is related to existence of two inequivalent sites for the same type of impurity ion. The difference between two g-factors is 0.03 that becomes only resolvable due to presence of the high field ALCs shown on the inset.

Interaction of WGMs with the REIs demonstrates the same structure as the previous experiments on Er doped YSO crystals at milliKelvin temperatures[7, 34, 50]. In particular, a corresponding map demonstrates four major transitions: two non-degenerate lattice sites with two

magnetically inequivalent subclasses (a) and (b) related by inversion[56, 57]. Additionally, the ^{167}Er isotope has nuclear magnetic moment $I = \frac{7}{2}$ providing an additional hyperfine structure both with zero and nonzero nuclear spin change.

In conclusion, WGM spectroscopy of Er:YSO and Eu:YSO at milliKelvin temperatures reveal additional impurities. Due to sufficient number of these impurities ions, the ensemble yields a strong coupling to WGMs at small fields. The coupling strength approaches 3.3 MHz overcoming typical spin linewidth of 1 – 2 MHz, which exceeds decay rates of SC quantum circuits. A spectroscopic map demonstrates ZFS attributed to Nickel and Chromium estimated to be present at the level of 100 ppb. These large ZFSs favour easier integration with SC qubits at smaller magnetic field. The measured g-factors reveal a strong anisotropy of these ions which is typical for an axial crystals. Intentional doping of these impurities could lead to significantly larger couplings, these experiments pave the way towards the use of IGI doped laser crystals for quantum memories and other Quantum Information Processing.

We thank L. Alegria and Z. Cole (Scientific Materials Corp.) for the valuable discussions concerning of spin impurity doping of YSO crystals. This work was supported by Australian Research Council grants CE110001013 and FL0992016 and by BMBF project QUIMP 01BQ1060.

* michael.tobar@uwa.edu.au

- [1] L. Tian, P. Rabl, R. Blatt, and P. Zoller, Phys. Rev. Lett. **92**, 247902 (2004).
- [2] A. Imamoglu, Phys. Rev. Lett. **102**, 083602 (2009).
- [3] J. Verdú, H. Zoubi, C. Koller, J. Majer, H. Ritsch, and J. Schmiedmayer, Phys. Rev. Lett. **103**, 043603 (2009).
- [4] Z.-L. Xiang, S. Ashhab, J. Q. You, and F. Nori, Reviews of Modern Physics **85**, 623 (2013).
- [5] C. Rigetti, J. M. Gambetta, S. Poletto, B. L. T. Plourde, J. M. Chow, A. D. Córcoles, J. A. Smolin, S. T. Merkel, J. R. Rozen, G. A. Keefe, M. B. Rothwell, M. B. Ketchen, and M. Steffen, Phys. Rev. B **86**, 100506 (2012).
- [6] H. Paik, D. I. Schuster, L. S. Bishop, G. Kirchmair, G. Catelani, A. P. Sears, B. R. Johnson, M. J. Reagor, L. Frunzio, L. I. Glazman, S. M. Girvin, M. H. Devoret, and R. J. Schoelkopf, Phys. Rev. Lett. **107**, 240501 (2011).
- [7] S. Probst, A. Tkalčec, H. Rotzinger, D. Rieger, J.-M. Le Floch, M. Goryachev, M. E. Tobar, A. V. Ustinov, and P. A. Bushev, Phys. Rev. B **90**, 100404 (2014).
- [8] J.-M. Le Floch, C. Bradac, N. Nand, S. Castelletto, M. E. Tobar, and T. Volz, Applied Physics Letters **105**, (2014).
- [9] J.-M. Le Floch, Y. Fan, M. Aubourg, D. Cros, N. C. Carvalho, Q. Shan, J. Bourhill, E. N. Ivanov, G. Humbert, V. Mdrangeas, and M. E. Tobar, Review of Scientific Instruments **84**, (2013).
- [10] M. Goryachev, W. Farr, D. Creedon, Y. Fan, M. Kostylev, and M. Tobar, arxiv.org/abs/1408.2905 (2014).
- [11] J. Miguel-Sánchez, A. Reinhard, E. Togan, T. Volz, A. Imamoglu, B. Besga, J. Reichel, and J. Estève, New Journal of Physics **15**, 045002 (2013).
- [12] G. Rempe, *Lasers and Electro-Optics 2009 and the European Quantum Electronics Conference. CLEO Europe - EQEC 2009. European Conference on, Lasers and Electro-Optics 2009 and the European Quantum Electronics Conference. CLEO Europe - EQEC 2009. European Conference on*, 1 (14-19 June 2009).
- [13] J. G. Hartnett, M. E. Tobar, A. Mann, E. N. Ivanov, and J. Krupka, IEEE Trans. on UFFC **46**, 993 (1999).
- [14] W. G. Farr, D. L. Creedon, M. Goryachev, K. Benmessai, and M. E. Tobar, Phys. Rev. B **88**, 224426 (2013).
- [15] M. Goryachev, W. G. Farr, and M. E. Tobar, Applied Physics Letters **103**, 262404 (2013).
- [16] M. Goryachev, W. G. Farr, D. L. Creedon, and M. E. Tobar, Phys. Rev. A **89**, 013810 (2014).
- [17] M. Goryachev, W. G. Farr, D. L. Creedon, and M. E. Tobar, Physical Review B **89**, 224407 (2014).
- [18] A. Schliesser, O. Arcizet, R. Riviere, G. Anetsberger, and T. J. Kippenberg, Nat Phys **5**, 509 (2009).
- [19] S. Forstner, S. Prams, E. D. Van Ooijen, J. D. Swaim, J. Knittel, G. I. Harris, A. Szorkovszky, H. Rubinszstein-Dunlop, and W. P. Bowen, *Quantum Electronics Conference & Lasers and Electro-Optics (CLEO/IQEC/PACIFIC RIM), 2011*, Quantum Electronics Conference & Lasers and Electro-Optics (CLEO/IQEC/PACIFIC RIM), 2011, 743 (Aug. 28 2011-Sept. 1 2011).
- [20] M. A. Taylor, J. Janousek, V. Daria, J. Knittel, B. Hage, H.-A. Bachor, and W. P. Bowen, Physical Review X **4**, 011017 (2014).
- [21] P. L. Stanwix, M. E. Tobar, P. Wolf, M. Susli, C. R. Locke, E. N. Ivanov, J. Winterflood, and F. van Kann, Phys. Rev. Lett. **95**, 040404 (2005).
- [22] J. Knittel, J. D. Swaim, D. L. McAuslan, G. A. Brawley, and W. P. Bowen, Sci. Rep. **3** (2013).
- [23] C. R. Locke, E. N. Ivanov, J. G. Hartnett, P. L. Stanwix, and M. E. Tobar, Review of Scientific Instruments **79**, (2008).
- [24] N. R. Nand, S. R. Parker, E. N. Ivanov, J.-M. Le Floch, J. G. Hartnett, and M. E. Tobar, *Applied Physics Letters*, Applied Physics Letters **103**, 043502 (Jul 2013).
- [25] P. Bourgeois, M. Oxborrow, M. Tobar, N. Bazin, Y. Kersalé, and V. Giordano, Applied Physics Letters **87**, 224104 (2005).
- [26] D. L. Creedon, K. Benmessai, M. E. Tobar, J. G. Hartnett, P. Bourgeois, Y. Kersale, J.-M. Le Floch, and V. Giordano, *Ultrasonics, Ferroelectrics and Frequency Control, IEEE Transactions on*, Ultrasonics, Ferroelectrics and Frequency Control, IEEE Transactions on **57**, 641 (March 2010).
- [27] J.-M. Le Floch, Y. Fan, G. Humbert, Q. Shan, D. Férachou, R. Bara-Maillet, M. Aubourg, J. G. Hartnett, V. Mdrangeas, D. Cros, J.-M. Blondy, J. Krupka, and M. E. Tobar, Review of Scientific Instruments **85**, (2014).
- [28] P. J. de Visser, D. J. Goldie, P. Diener, S. Withington, J. J. A. Baselmans, and T. M. Klapwijk, Physical Review Letters **112**, 047004 (2014).
- [29] A. Megrant, C. Neill, R. Barends, B. Chiaro, Y. Chen, L. Feigl, J. Kelly, E. Lucero, M. Mariantoni, P. J. J. O'Malley, D. Sank, A. Vainsencher, J. Wenner, T. C. White, Y. Yin, J. Zhao, C. J. Palmström, J. M. Martinis, and A. N. Cleland, Applied Physics Letters **100**, (2012).

- [30] D. L. Creedon, Y. Reshitnyk, W. Farr, J. M. Martinis, T. L. Duty, and M. E. Tobar, *Applied Physics Letters* **98**, (2011).
- [31] J. Bourhill, K. Benmessai, M. Goryachev, D. L. Creedon, W. Farr, and M. E. Tobar, *Phys. Rev. B* **88**, 235104 (2013).
- [32] N. Carvalho, J.-M. L. Floch, J. Krupka, and M. E. Tobar, arXiv (2015).
- [33] T. Böttger, C. W. Thiel, Y. Sun, and R. L. Cone, *Phys. Rev. B* **73**, 075101 (2006).
- [34] P. Bushev, A. K. Feofanov, H. Rotzinger, I. Protopopov, J. H. Cole, C. M. Wilson, G. Fischer, A. Lukashenko, and A. V. Ustinov, *Physical Review B* **84**, 060501 (2011).
- [35] M. P. Hedges, J. J. Longdell, Y. Li, and M. J. Sellars, *Nature* **465**, 1052 (2010).
- [36] C. Clausen, I. Usmani, F. Bussieres, N. Sangouard, M. Afzelius, H. de Riedmatten, and N. Gisin, *Nature* **469**, 508 (2011).
- [37] Q.-F. Chen, A. Troshyn, I. Ernsting, S. Kayser, S. Vasilyev, A. Nevsky, and S. Schiller, *Phys. Rev. Lett.* **107**, 223202 (2011).
- [38] G. Wolfowicz, H. Maier-Flaig, R. Marino, A. Ferrier, H. Vezin, J. Morton, and P. Goldner, arXiv:1412.7298 (2014).
- [39] S. Probst, H. Rotzinger, A. Ustinov, and P. Bushev, arXiv:1501.01499 (2015).
- [40] C. O'Brien, N. Lauk, S. Blum, G. Morigi, and M. Fleischhauer, *Phys. Rev. Lett.* **113**, 063603 (2014).
- [41] L. Williamson, Y.-H. Chen, and J. Longdell, arxiv.org/abs/1403.1608 (2014).
- [42] K. Stannigel, P. Rabl, A. S. Sørensen, P. Zoller, and M. D. Lukin, *Phys. Rev. Lett.* **105**, 220501 (2010).
- [43] A. M. Stephens, J. Huang, K. Nemoto, and W. J. Munro, *Phys. Rev. A* **87**, 052333 (2013).
- [44] D. V. Strekalov, H. G. L. Schwefel, A. A. Savchenkov, A. B. Matsko, L. J. Wang, and N. Yu, *Phys. Rev. A* **80**, 033810 (2009).
- [45] Y.-K. Kuo, M. Huang, and M. Birnbaum, *Quantum Electronics, IEEE Journal of, Quantum Electronics, IEEE Journal of* **31**, 657 (Apr 1995).
- [46] Y. Kubo, C. Grezes, A. Dewes, T. Umeda, J. Isoya, H. Sumiya, N. Morishita, H. Abe, S. Onoda, T. Ohshima, V. Jacques, A. Dréau, J.-F. Roch, I. Diniz, A. Auffeves, D. Vion, D. Esteve, and P. Bertet, *Phys. Rev. Lett.* **107**, 220501 (2011).
- [47] K. Henschel, J. Majer, J. Schmiedmayer, and H. Ritsch, *Physics Review A* **82**, 033810 (2010).
- [48] A. Wallraff, D. I. Schuster, A. Blais, L. Frunzio, R. S. Huang, J. Majer, S. Kumar, S. M. Girvin, and R. J. Schoelkopf, *Nature* **431**, 162 (2004).
- [49] S. Saito, X. Zhu, R. Amsüss, Y. Matsuzaki, K. Kakuyanagi, T. Shimo-Oka, N. Mizuochi, K. Nemoto, W. J. Munro, and K. Semba, *Phys. Rev. Lett.* **111**, 107008 (2013).
- [50] S. Probst, H. Rotzinger, S. Wünsch, P. Jung, M. Jerger, M. Siegel, A. V. Ustinov, and P. A. Bushev, *Physical Review Letters* **110**, 157001 (2013).
- [51] R. R. Rakhimov, H. D. Horton, and G. B. Loutts, *MRS Online Proceedings Library* **560**, null (1999).
- [52] R. R. Rakhimov, H. D. Horton, D. E. Jones, G. B. Loutts, and H. R. Ries, *Chemical Physics Letters* **319**, 639 (2000).
- [53] R. D. Shannon, *Acta Crystallographica Section A* **32**, 751 (1976).
- [54] Y. Q. Jia, *Journal of Solid State Chemistry* **95**, 184 (1991).
- [55] C. Poole and H.A.Farach, *Handbook of Electron Spin Resonance*, Vol. 2 (Springer-Verlag, NY, 1999).
- [56] Y. Sun, T. Böttger, C. W. Thiel, and R. L. Cone, *Physical Review B* **77**, 085124 (2008).
- [57] R. Amsüss, C. Koller, T. Nöbauer, S. Putz, S. Rotter, K. Sandner, S. Schneider, M. Schramböck, G. Steinhäuser, H. Ritsch, J. Schmiedmayer, and J. Majer, *Physical Review Letters* **107**, 060502 (2011).